Electronic Supplementary Material (ESI) for Dalton Transactions

The First Enantiopure Lanthanoid Cryptate

Tuba Güden-Silber,[†] Christine Doffek,[†] Carlos Platas-Iglesias,[‡*] and Michael Seitz[†*]

[†] Inorganic Chemistry I, Department of Chemistry and Biochemistry, Ruhr-University Bochum, 44780 Bochum, Germany.

[‡] Departamento de Química Fundamental, Universidade da Coruña, Campus da Zapateira-Rúa da Fraga 10, 15008 A Coruña, Spain.

Email: carlos.platas.iglesias@udc.es, michael.seitz@rub.de

Supporting Information

Table of Contents Page

1 Synthesis

Chemicals were purchased from commercial suppliers and used as received unless stated otherwise. Deuterated solvents had deuterium contents > 99.8%D and were used as commercially available without additional purification or drying procedures. CH_3CN for the synthesis of the cryptates was HPLC-grade. Other solvents were dried by standard procedures (CH_2Cl_2: CaH_2). Air-sensitive reactions were carried out under a dry, dioxygen-free atmosphere of N_2 using the Schlenk technique. Column chromatography was performed with silica gel 60 (Merck, 0.063-0.200 mm). Analytical thin layer chromatography (TLC) was done on silica gel 60 F_{254} plates (Merck, coated on aluminium sheets). Overall deuteration levels were established by deconvolution of the corresponding mass spectra. ESI mass spectrometry was done using a Bruker Daltonics Esquire6000 spectrometer. NMR spectra were measured on Bruker DPX-250 (^{1}H: 250 MHz, ^{13}C: 62.9 MHz) and Bruker DPX-200 (^{1}H: 200 MHz, ^{13}C: 50.3 MHz) instruments.

N,N'-Dioxide 4

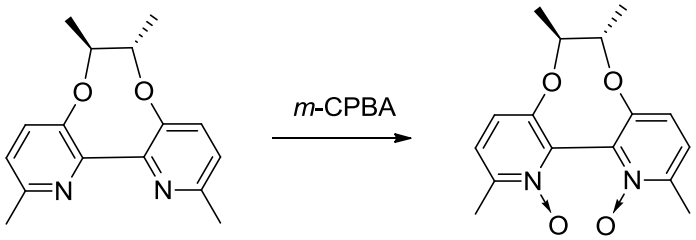

3 **4**

The starting material **3**[1] (0.25 g, 0.92 mmol, 1.0 equiv.) was dissolved in $CHCl_3$ (25 mL) and the solution was cooled in an ice-bath. A solution of *m*-chloroperbenzoic acid (0.62 g of 77wt%, 0.48 g pure, 2.77 mmol, 3.0 equivs.) in $CHCl_3$ (15 mL) was added dropwise in the course of 20 min. The solution was allowed to reach room temperature over ca. 2 h and was stirred overnight. The mixture was extracted with saturated aq. Na_2CO_3 solution (20 mL) and the organic phase was dried ($MgSO_4$). After evaporation of the solvent under reduced pressure, the resulting solid was purified by column chromatography (SiO_2, gradient: CH_2Cl_2 / MeOH 100:1 $\rightarrow$ 9:1). The product was obtained as a colorless solid (0.22 g, 79%).

Mp > 200°C. ^{1}H NMR (250 MHz, $CDCl_3$): δ = 7.24 (d, J = 8.5 Hz, 2 H), 6.93 (d, J = 8.5 Hz, 2 H), 3.84-3.69 (m, 2 H), 2.47 (s, 6 H), 1.29 (d, J = 6.0 Hz, 6 H) ppm. ^{13}C NMR (62.9 MHz, $CDCl_3$): δ = 156.3, 146.0, 137.2, 126.2, 86.6, 18.8, 17.5 ppm. MS (ESI+): m/z (%) = 302.95 (26, $[M+H]^+$), 324.89 (100, $[M+Na]^+$). TLC: R_f = 0.28 (SiO_2, CH_2Cl_2/MeOH 9:1, detection: UV).

Dibromide 5

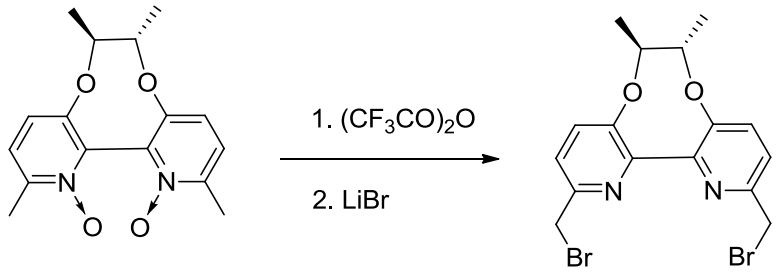

4 **5**

Under N_2, the starting material **4** (0.21 g, 0.69 mmol, 1.0 equiv.) was dissolved in dry CH_2Cl_2 (8 mL), trifluoroacetic acid anhydride (7.0 mL, 10.6 g, 50.4 mmol, 73 equivs.) was added, and the solution was heated under reflux for 3 h. Volatiles were removed under reduced pressure ($p \approx 0.4$ mbar) and the remaining pale-yellow oil was dissolved in an icecold mixture of dry THF (6 mL) and dry DMF (2 mL). Anhydrous LiBr (1.04 g, 12.0 mmol, 17.4 equivs.) was added in portions and the solution was stirred at ambient temperature for 26 h. Volatiles were removed under reduced pressure (bath temperature 50°C) and the remaining material was partitioned between CH_2Cl_2 (50 mL) and water (30 mL). The organic phase was isolated, dried ($MgSO_4$), and concentrated. The oily residue was subjected to column chromatography (SiO_2, hexanes/EtOAc 1:1). The product was obtained as a colorless oil (0.13 g, 44%) that turned increasingly purple on standing at room temperature in the course of a few days. It was consequently stored at –20°C or directly converted to **6**.

^{1}H NMR (200 MHz, $CDCl_3$): δ = 7.55 (d, J = 8.4 Hz, 2 H), 7.46 (d, J = 8.4 Hz, 2 H), 4.66 (s, 4 H), 3.95-3.80 (m, 2 H), 1.33 (d, J = 5.7 Hz, 6 H) ppm. ^{13}C NMR (50.3 MHz, $CDCl_3$): δ = 154.8, 152.6, 146.9, 132.2, 126.1, 85.2, 32.8, 18.7 ppm. MS (ESI+): m/z (%) = 451.76 (100, $[M+Na]^+$, Br_2 pattern). R_f = 0.23 (SiO_2, CH_2Cl_2/MeOH 100:1, detection: UV).

Dibromide *N,N′*-Dioxide 6

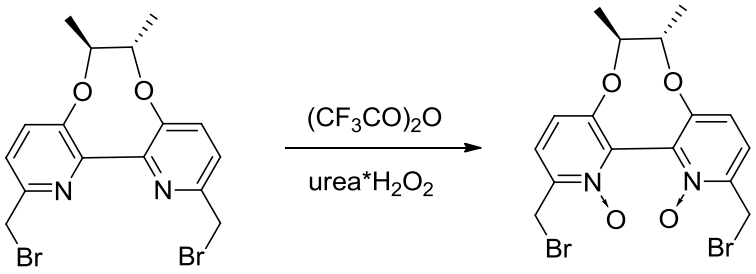

5 **6**

Under N_2, the starting material **5** (0.13 g, 0.30 mmol, 1.0 equiv.) was dissolved in dry CH_2Cl_2 (5 mL), cooled in an ice-bath and urea-hydrogen peroxide adduct (0.12 g, 1.28 mmol, 4.2 equivs.) was added in portions. Trifluoroacetic acid anhydride (0.18 mL, 0.27 g, 1.28 mmol, 4.2 equivs.) was added dropwise, the mixture was allowed to come to room temperature over the course of ca. 1 h and was stirred for additional 22 h. The solution was diluted with CH_2Cl_2 (10 mL), a saturated aqueous solution of sodium thiosulfate pentahydrate (3 mL) was added and the biphasic mixture was vigorously stirred for 5 min. The organic phase was isolated, dried ($MgSO_4$), and concentrated under reduced pressure. The remaining residue was subjected to column chromatography (SiO_2, gradient: CH_2Cl_2/MeOH 100:1 → 25:1). The product was obtained as a colorless oil (0.13 g, 94%).

Mp 128-130°C (decomp.). ^{1}H NMR (200 MHz, $CDCl_3$): δ = 7.61 (d, *J* = 8.7 Hz, 2 H), 7.07 (d, *J* = 8.7 Hz, 2 H), 4.92 (d, *J* = 11.3 Hz, 2 H), 4.55 (d, *J* = 11.3 Hz, 2 H), 4.04-3.76 (m, 2 H), 1.41 (d, *J* = 6.1 Hz, 6 H) ppm. ^{13}C NMR (50.3 MHz, $CDCl_3$): δ = 158.1, 144.1, 137.4, 127.0, 118.7, 86.8, 25.7, 18.8 ppm. MS (ESI+): m/z (%) = 482.74 (100, $[M+Na]^+$, Br_2 pattern). R_f = 0.50 (SiO_2, CH_2Cl_2/MeOH 9:1, detection: UV).

Sodium Cryptate 8-Na

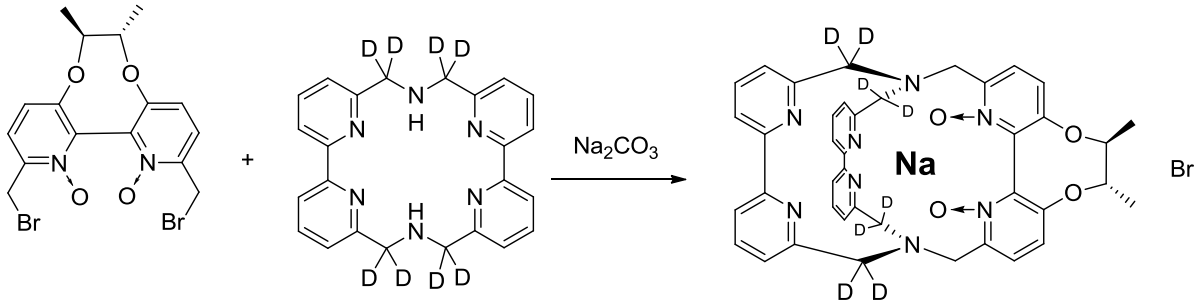

6 **7** **8-Na**

The dibromide **6** (89 mg, 193 µmol 1.0 equiv.) was added to a solution of the macrocycle **7**[2] (78 mg, 193 µmol 1.0 equiv.) and anhydrous Na_2CO_3 (205 mg, 1.93 mmol, 10 equivs.) in dry CH_3CN (100 ml). The mixture was heated under reflux for 48 h, filtered while hot, and the filtrate was concentrated. The residue was subjected to column chromatography (SiO_2,

CH_2Cl_2/MeOH gradient 24:1 → 9:1, detection: UV and I_2 vapor) to yield a colorless solid (49 mg, 32%, 98.8%D).

^{1}H NMR (250 MHz, CD_2Cl_2): δ = 7.96-7.54 (m, 10 H), 7.51-7.32 (m, 4 H), 7.15 (d, *J* = 8.5 Hz, 2 H), 4.23 (d, *J* = 12.0 Hz, 2 H), 4.06-3.76 (m, 2 H), 3.33 (d, *J* = 12.0 Hz, 2 H), 1.33 (d, *J* = 6.0 Hz, 6 H) ppm. ^{13}C NMR (62.9 MHz, CD_2Cl_2): δ = 159.2, 158.3, 157.7, 157.6, 156.9, 144.8, 139.0, 138.7, 138.3, 128.9, 125.0, 124.9, 122.6, 121.8, 120.0, 86.8, 61.2-59.2 (m), 54.7, 19.1 ppm. MS (ESI+): m/z (%) = 723.13 (100, $[M]^+$). R_f = 0.25 (SiO_2, CH_2Cl_2/MeOH 9:1, detection: UV). $[\alpha]_D^{20}$ = –237 (c = 0.40, MeOH).

Ytterbium Cryptate 9-Yb

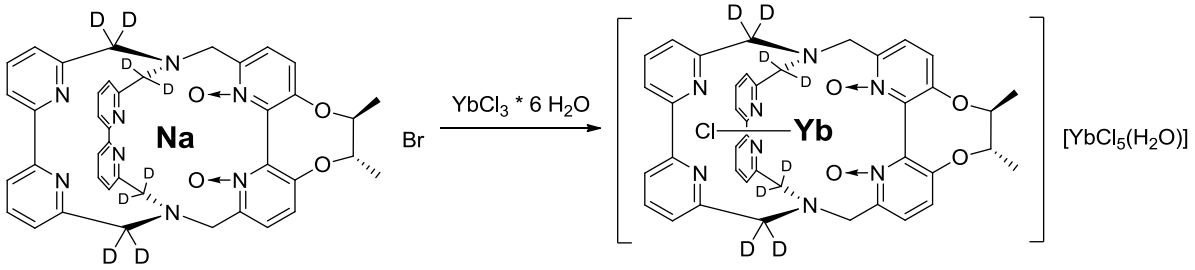

8-Na **9-Yb**

The sodium cryptate **8-Na** (11.3 mg, 14.1 µmol, 1.0 equiv.) was dissolved in dry CH_3CN (5 mL) and $YbCl_3 \cdot 6\ H_2O$ (8.2 mg, 21.1 µmol, 1.5 equivs.) was added. The mixture was heated under reflux for 40 h. The solvent was removed and the residue was dissolved in a minimum of MeOH. The solution was layered with Et_2O until the mixture became turbid. After storing the mixture at 4°C overnight, the precipitate was collected on a membrane filter, washed with Et_2O and dried under reduced pressure. The complex was obtained as a colorless solid (9.4 mg, 52%).

^{1}H NMR (250 MHz, CD_3OD): δ = 62.4 (s, 2 H), 30.6 (s, 2 H), 15.7 (s, 2 H), 12.2 (s, 2 H), 9.76 (s, 2 H), 4.01 (s, 2 H), –3.86 (s, 6 H), –5.22 (s, 2 H), –6.04 (s, 2 H), –12.7 (s, 2H), –75.8 (s, 2 H) ppm. MS (ESI+): m/z (%) = 454.98 ($[M]^{2+}$).

The ^{1}H NMR spectra (250 MHz) in the enantiopure solvents methyl L-lactate (Sigma-Aldrich, 97%ee) and methyl D-lactate (Sigma-Aldrich, 96%ee) were measured by dissolving 1.0 mg of **9-Yb** in a mixture of 0.66 mL of the respective lactate and 0.06 mL CD_2Cl_2 (lock), followed by addition of one drop of tetramethylsilane.

Lutetium Cryptate 9-Lu

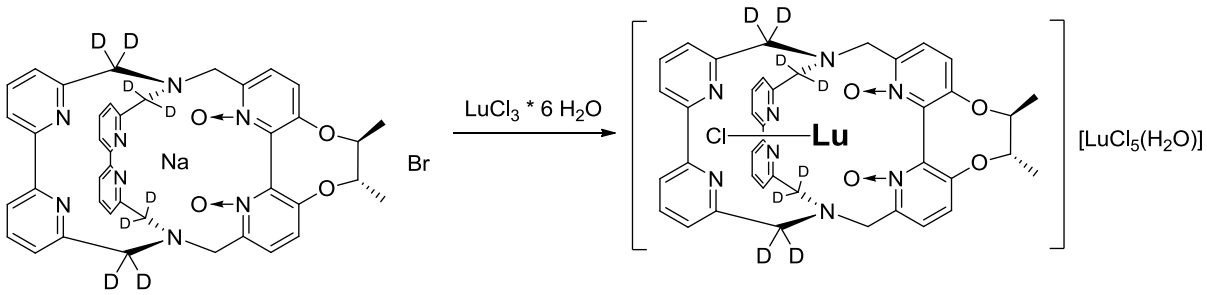

8-Na **9-Lu**

The sodium cryptate **8-Na** (19.2 mg, 23.9 µmol, 1.0 equiv.) was dissolved in dry CH_3CN (8 mL) and $LuCl_3 \cdot 6\ H_2O$ (14.0 mg, 35.8 µmol, 1.5 equivs.) was added. The mixture was heated under reflux for 40 h. The solvent was removed and the residue was dissolved in a minimum of MeOH. The solution was layered with Et_2O until the mixture became turbid. After storing the mixture at 4°C overnight, the precipitate was collected on a membrane filter, washed with Et_2O and dried under reduced pressure. The complex was obtained as a colorless solid (19.3 mg, 63%).

^{1}H NMR (250 MHz, CD_3OD): δ = 8.60-8.31 (m, 4 H), 8.30-8.00 (m, 8 H), 7.77-7.54 (m, 4 H), 4.66 (d, *J* = 12.5 Hz, 2 H), 4.34-4.11 (m, 2 H), 3.91 (d, *J* = 12.5 Hz, 2 H), 1.60-1.30 (m, 6 H) ppm. MS (ESI+): m/z (%) = 454.46 ($[M]^{2+}$).

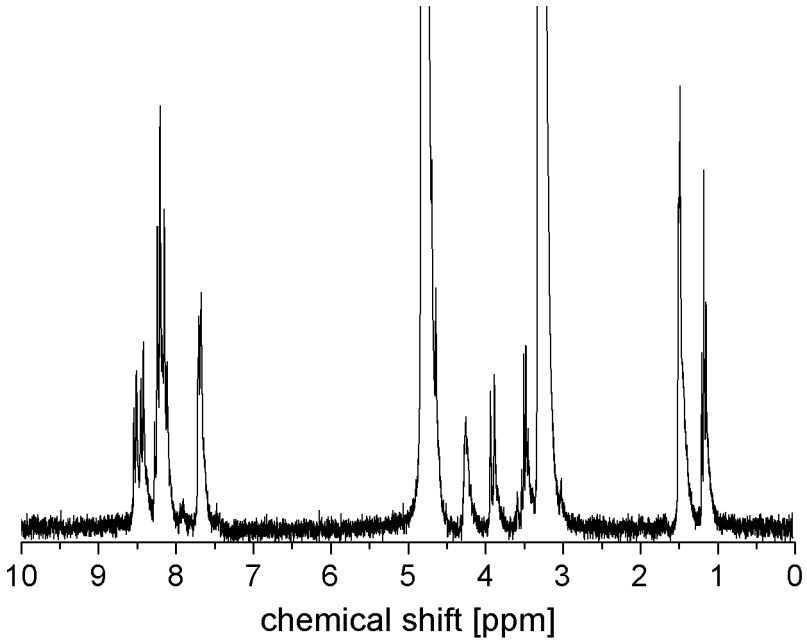

Figure S1. ^{1}H-NMR (250 MHz, CD_3OD) of **9-Lu**.

2 HPLC

Analytical reversed-phase HPLC was performed on a Lichrospher RP-18e analytical column (Merck, 125×4mm-5μm, flow rate: 1 mL min^{-1}, UV detection: 300 nm) under the following conditions:

Mobile Phases: A: H_2O (+1% TFA, v/v) B: CH_3CN (HPLC gradient grade)

Gradient:

min	%A	%B
0	70	30
5	70	30
20	5	95
25	5	95
35	70	30
40	70	30

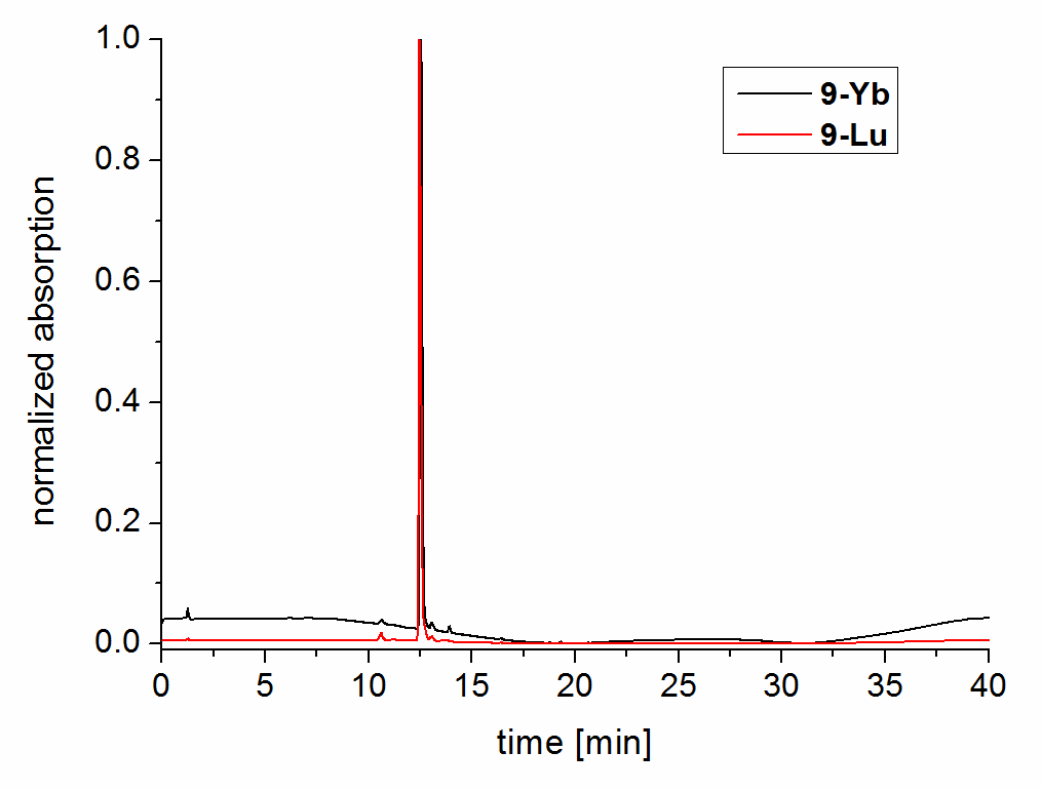

Figure S2. HPLC traces of **9-Ln**.

3 DFT Calculations

All calculations were performed employing DFT within the hybrid meta generalized gradient approximation (hybrid meta-GGA), with the TPSSh exchange-correlation functional,[3] and the Gaussian 09 package (Revision A.02).[4] Full geometry optimizations of the diastereomers of **9-Yb** were performed in solution by using the large-core relativistic effective core potential (LCRECP) of Dolg *et al.* and the related [5s4p3d]-GTO valence basis set for the lanthanoids,[5] and the standard 6-31G(d,p) basis set for C, H, Cl, N and O atoms. This LCRECP includes 46+4f^{n} electrons in the core for the Ln^{III} ion, leaving the outermost 8 electrons to be treated explicitly. The use of LCRECP has been justified by the fact that 4f orbitals do not significantly contribute to bonding due to their limited radial extension as compared to the 5d and 6s shells.[6,7] LCRECP calculations were shown to provide good results in DFT studies that focus on the structure and dynamics, or the estimates of relative energies, of Ln^{III} complexes.[8] No symmetry constraints were imposed during the optimizations. The default values for the integration grid ("fine") and the SCF energy convergence criteria (10^{-8}) were used. The stationary points found on the potential energy surfaces as a result of the geometry optimizations have been tested to represent energy minima rather than saddle points via frequency analysis. The calculated relative free energies of the two isomers include non-potential energy contributions (zero point energies and thermal terms) obtained from frequency calculations.

Solvent effects (methanol, ε = 32.613) were evaluated by using the polarizable continuum model (PCM), in which the solute cavity is built as an envelope of spheres centered on atoms or atomic groups with appropriate radii. In particular, we used the integral equation formalism (IEFPCM) variant as implemented in Gaussian 09.[9]

(S,S,S_a)-9-Yb, TPSSh/LCRECP/6-31G(d,p) (0 imaginary frequencies)

Center Number	Atomic Number	Coordinates (Angstroms) X	Y	Z
1	70	1.093045	0.000005	-0.000002
2	7	2.055238	0.767714	-2.257825
3	6	2.442787	2.041824	-2.475344
4	6	3.238288	2.387676	-3.576850
5	6	3.625010	1.397851	-4.475938
6	6	3.212672	0.085870	-4.255304
7	6	2.437653	-0.184429	-3.127424
8	6	1.999639	-1.581528	-2.786881
9	7	1.417266	2.559697	-0.344349
10	6	2.011080	3.037697	-1.470362
11	6	2.211520	4.407639	-1.677107
12	6	1.832053	5.314326	-0.692115
13	6	1.243936	4.827571	0.469034
14	6	1.035913	3.450756	0.593116
15	7	0.656691	-1.556228	-2.151683
16	6	0.275268	2.935981	1.784459
17	6	-1.695005	-1.005536	-2.556844
18	7	-1.835011	-0.242239	-1.433949
19	6	-2.936503	-0.361883	-0.630966
20	6	-4.017916	-1.160547	-1.037624
21	6	-2.772543	-1.771983	-2.990944
22	6	-3.957169	-1.833317	-2.260489
23	6	-0.325986	-1.015887	-3.151748
24	8	-0.889810	-0.633099	1.130498
25	1	3.565730	3.407210	-3.730785
26	1	4.237650	1.648908	-5.334854
27	1	3.484110	-0.714634	-4.934069
28	1	2.001373	-2.217912	-3.682159
29	1	2.703702	-2.011845	-2.064093
30	1	2.655599	4.768137	-2.595190
31	1	1.993058	6.377589	-0.831669
32	1	0.934077	5.492879	1.266942
33	1	0.398169	3.621461	2.634232
34	1	-0.786882	2.941420	1.521074
35	1	-0.329399	-1.633323	-4.057857
36	1	-0.015575	-0.002757	-3.411483
37	7	2.055235	-0.767700	2.257825
38	6	2.442805	-2.041803	2.475348
39	6	3.238309	-2.387642	3.576855
40	6	3.625013	-1.397810	4.475943
41	6	3.212657	-0.085835	4.255305
42	6	2.437636	0.184451	3.127422
43	6	1.999605	1.581543	2.786876
44	7	0.656652	1.556225	2.151686
45	6	-0.326011	1.015885	3.151762
46	6	-1.695029	1.005523	2.556858
47	7	-1.835024	0.242214	1.433967
48	6	-2.936510	0.361856	0.630974
49	6	0.275329	-2.935994	-1.784465
50	6	1.035976	-3.450759	-0.593119
51	7	1.417306	-2.559694	0.344348
52	8	-0.889802	0.633078	-1.130461
53	6	2.011120	-3.037684	1.470365
54	6	2.211585	-4.407622	1.677113
55	6	1.832139	-5.314315	0.692118
56	6	1.244021	-4.827570	-0.469034
57	1	0.934176	-5.492885	-1.266943

58	1	1.993163	-6.377576	0.831673
59	1	2.655668	-4.768110	2.595197
60	1	0.398245	-3.621468	-2.634240
61	1	-0.786821	-2.941454	-1.521082
62	6	-4.017929	1.160517	1.037624
63	6	-3.957193	1.833295	2.260483
64	6	-2.772569	1.771971	2.990945
65	1	-0.329423	1.633332	4.057862
66	1	-0.015587	0.002760	3.411505
67	1	2.001338	2.217931	3.682151
68	1	2.703658	2.011865	2.064082
69	1	3.484082	0.714675	4.934068
70	1	4.237655	-1.648856	5.334861
71	1	3.565764	-3.407172	3.730792
72	1	-4.786455	2.449015	2.587252
73	1	-2.653979	2.353935	3.897360
74	1	-4.786425	-2.449041	-2.587266
75	1	-2.653946	-2.353941	-3.897362
76	17	3.817621	0.000016	0.000000
77	8	-5.043092	-1.328902	-0.162111
78	8	-5.043101	1.328889	0.162106
79	6	-6.303298	-0.625627	-0.440983
80	6	-6.303294	0.625571	0.440918
81	1	-6.303169	-0.329467	-1.495342
82	1	-6.303136	0.329312	1.495247
83	6	-7.433449	1.597301	0.140645
84	1	-8.401555	1.130288	0.338256
85	1	-7.341584	2.480880	0.776020
86	1	-7.401941	1.911524	-0.906683
87	6	-7.433442	-1.597353	-0.140655
88	1	-7.401937	-1.911521	0.906688
89	1	-8.401551	-1.130356	-0.338296
90	1	-7.341572	-2.480964	-0.775985

E(RTPSSh) = -2784.58334050 Hartree
Zero-point correction = 0.712448
Thermal correction to Energy = 0.755983
Thermal correction to Enthalpy = 0.756927
Thermal correction to Gibbs Free Energy = 0.639823
Sum of electronic and zero-point Energies = -2783.870893
Sum of electronic and thermal Energies = -2783.827358
Sum of electronic and thermal Enthalpies = -2783.826414
Sum of electronic and thermal Free Energies = -2783.943517

(S,S,R_a)-9-Yb, TPSSh/LCRECP/6-31G(d,p) (0 imaginary frequencies)

Center Number	Atomic Number	Coordinates (Angstroms) X	Y	Z
1	70	-1.055285	0.000000	0.000001
2	7	-2.026898	0.686652	-2.284880
3	6	-2.418203	1.950038	-2.551484
4	6	-3.213978	2.251274	-3.665609
5	6	-3.600965	1.225636	-4.523639
6	6	-3.188788	-0.076518	-4.250096
7	6	-2.410888	-0.300130	-3.114076
8	6	-1.968428	-1.680509	-2.716796
9	7	-1.388102	2.544138	-0.446039
10	6	-1.990925	2.982176	-1.582809
11	6	-2.205280	4.343309	-1.829676
12	6	-1.827237	5.282656	-0.875194
13	6	-1.227018	4.836777	0.296545
14	6	-1.008466	3.466096	0.461092
15	7	-0.629136	-1.621438	-2.074511
16	6	-0.238821	2.986412	1.660517
17	6	1.723393	-1.091717	-2.503291
18	7	1.892717	-0.286069	-1.414325
19	6	3.014563	-0.376563	-0.625087
20	6	4.083370	-1.194966	-1.038449
21	6	2.771979	-1.904063	-2.919782
22	6	3.966737	-1.946566	-2.211326
23	6	0.351608	-1.105337	-3.088697
24	8	0.952038	-0.601451	1.131909
25	1	-3.541007	3.263923	-3.860821
26	1	-4.214132	1.441619	-5.391684
27	1	-3.461929	-0.904304	-4.894556
28	1	-1.958305	-2.350883	-3.586714
29	1	-2.675052	-2.087478	-1.983111
30	1	-2.660030	4.671526	-2.754614
31	1	-1.998799	6.339741	-1.045673
32	1	-0.917433	5.528512	1.071726
33	1	-0.347414	3.698599	2.489756
34	1	0.820129	2.974115	1.385233
35	1	0.347351	-1.743041	-3.980761
36	1	0.045482	-0.096523	-3.368776
37	7	-2.026889	-0.686653	2.284884
38	6	-2.418185	-1.950041	2.551490
39	6	-3.213953	-2.251280	3.665621
40	6	-3.600943	-1.225642	4.523650
41	6	-3.188776	0.076513	4.250102
42	6	-2.410881	0.300128	3.114079
43	6	-1.968428	1.680509	2.716796
44	7	-0.629137	1.621441	2.074509
45	6	0.351611	1.105348	3.088694
46	6	1.723395	1.091727	2.503286
47	7	1.892722	0.286065	1.414331
48	6	3.014569	0.376546	0.625092
49	6	-0.238817	-2.986409	-1.660521
50	6	-1.008458	-3.466094	-0.461093
51	7	-1.388088	-2.544137	0.446043
52	8	0.952037	0.601448	-1.131896
53	6	-1.990908	-2.982178	1.582812
54	6	-2.205265	-4.343311	1.829677
55	6	-1.827229	-5.282656	0.875191
56	6	-1.227014	-4.836774	-0.296549
57	1	-0.917436	-5.528508	-1.071735

58	1	-1.998793	-6.339741	1.045668
59	1	-2.660012	-4.671529	2.754616
60	1	-0.347413	-3.698595	-2.489760
61	1	0.820134	-2.974112	-1.385240
62	6	4.083377	1.194952	1.038448
63	6	3.966735	1.946576	2.211309
64	6	2.771978	1.904083	2.919766
65	1	0.347354	1.743058	3.980754
66	1	0.045490	0.096535	3.368781
67	1	-1.958306	2.350884	3.586713
68	1	-2.675055	2.087474	1.983112
69	1	-3.461920	0.904300	4.894561
70	1	-4.214104	-1.441628	5.391698
71	1	-3.540974	-3.263931	3.860836
72	1	4.774689	2.601255	2.512245
73	1	2.622893	2.528692	3.792494
74	1	4.774693	-2.601234	-2.512280
75	1	2.622897	-2.528655	-3.792523
76	17	-3.779752	-0.000010	0.000005
77	8	5.155562	-1.342687	-0.219682
78	8	5.155570	1.342686	0.219685
79	6	6.393142	-0.586747	-0.492438
80	6	6.393150	0.586747	0.492418
81	1	7.186138	-1.287245	-0.219233
82	1	7.186147	1.287234	0.219189
83	6	6.557155	-0.149040	-1.939074
84	1	7.535034	0.331456	-2.036845
85	1	6.535181	-0.998579	-2.625046
86	1	5.790585	0.573594	-2.230327
87	6	6.557208	0.149057	1.939059
88	1	7.535078	-0.331461	2.036806
89	1	6.535276	0.998610	2.625013
90	1	5.790629	-0.573550	2.230356

E(RTPSSh) = -2784.57567050 Hartree
Zero-point correction = 0.713058
Thermal correction to Energy = 0.756245
Thermal correction to Enthalpy = 0.757189
Thermal correction to Gibbs Free Energy = 0.641179
Sum of electronic and zero-point Energies = -2783.862613
Sum of electronic and thermal Energies = -2783.819425
Sum of electronic and thermal Enthalpies = -2783.818481
Sum of electronic and thermal Free Energies = -2783.934492

4 Lanthanoid Induced Shift Analysis

The binding of a ligand to the paramagnetic Yb^{III} ion provokes relatively large NMR frequency shifts at the ligand nuclei, with magnitudes and signs depending on the location of the nucleus relative to the metal centre.[8] The isotropic paramagnetic shift induced by Yb^{III} (δ_i^{para}) are considered to be largely pseudocontact in origin, and they can be approximated by the following equation:

$$\delta_i^{dip} = D_1 \frac{3\cos^2\theta - 1}{r^3} + D_2 \frac{\sin^2\theta \cos 2\varphi}{r^3} \qquad (1)$$

where r, θ and φ are the spherical coordinates of the observed nucleus with respect to Yb^{III} at the origin and D_1 and D_2 are proportional, respectively, to the axial [χ_{zz} – 1/3(χ_{xx} + χ_{yy} + χ_{zz})] and rhombic (χ_{xx} - χ_{yy}) anisotropies of the magnetic susceptibility tensor χ. In the special case of axial symmetry, that is, if the molecule presents a symmetry axis C_n with n ≥ 3, the second term of Equation (1) vanishes since D_2 = 0. The diamagnetic contribution to the observed chemical shifts can be accounted for by measuring the ^{1}H NMR shifts for the corresponding diamagnetic Lu(III) cryptate.

The DFT optimized geometries of the (*S,S,S*$_a$) and (*S,S,R*$_a$) isomers of **9-Yb** were used to assess the agreement between the experimental and predicted Yb(III)-induced paramagnetic shifts as predicted by Equation (1). Table S1 shows the D_1 and D_2 values providing the best fit of the experimental shift values, as well as a comparison of the experimental and calculated paramagnetic shifts according to the dipolar model. The agreement between the experimental and calculated isotropic shifts obtained by using the (*S,S,S*$_a$) isomer was very good (AF_j = 0.0176, Table S1), while a poorer agreement factor was obtained for the (*S,S,R*$_a$) form (AF_j = 0.0552). The better agreement between the experimental shifts and those calculated for the (*S,S,S*$_a$) isomer is clearly confirmed by Figure S1, which shows the differences between experimental and theoretical LIS values (Δδ = $|\delta_i^{exp} - \delta_i^{cal}|$) for the (*S,S,S*$_a$) and (*S,S,R*$_a$) forms. There are obviously larger deviations from the experimental values for most proton nuclei of the (*S,S,R*$_a$) form than for the same nuclei in the (*S,S,S*$_a$) one. In particular, larger deviations from the experimental values are observed for protons H6o and H7o in the case of the (*S,S,R*$_a$) isomer. These results unambiguously prove that the isomer observed in solution for **9-Yb** corresponds to the (*S,S,S*$_a$) enantiomer, in agreement with the relative free energies obtained by DFT calculations. As expected for a non-axial system the calculated D_1 and D_2 values define a rhombic magnetic susceptibility tensor.

Table S1. Chemical shifts (ppm with respect to TMS) observed for **9-Lu** and comparison of experimental and calculated ^{1}H Shifts for **9-Yb**.[a]

	Lu	Yb	Yb	Yb
	δ_i^{exp}	δ_i^{exp}	$\delta_i^{calc}(S,S,S_a)^b$	$\delta_i^{calc}(S,S,R_a)^b$
H1o	3.91	-75.78	-76.06	-76.91
H2o	4.66	15.67	16.57	16.41
H3o	8.20	12.18	12.12	13.08
H4o	8.20	4.01	4.51	5.08
H6o	4.25	-6.04	-5.40	-2.34
H7o	1.19	-3.86	-3.81	-6.86
H3b	7.70	-5.22	-6.00	-5.08
H4b	8.53	-12.74	-11.81	-11.05
H5b	8.20	-13.65	-13.58	-13.15
H6b	8.20	9.76	10.14	9.67
H7b	8.44	30.59	30.88	29.93
H8b	7.70	62.44	61.88	60.19
D_1^c			2150 ± 31	2078 ± 117
D_2^c			-7931 ± 32	-7676 ± 160
AF_i^d			0.0176	0.0552

[a] The diamagnetic contribution was estimated from the shifts observed for the Lu^{III} analogue. [b] Values calculated by using Eq. (1) and the structures of 9-Yb optimized at the TPSSh/LCRECP/6-31G(d,p) level. [c] In ppm·Å^{-3}.

[d] $AF_j = [\sum_i (\delta_i^{exp} - \delta_i^{cal})^2 / \sum_i (\delta_i^{exp})^2]^{1/2}$, where δ_i^{exp} and δ_i^{cal} represent the experimental and calculated values of a nucleus *i*, respectively.

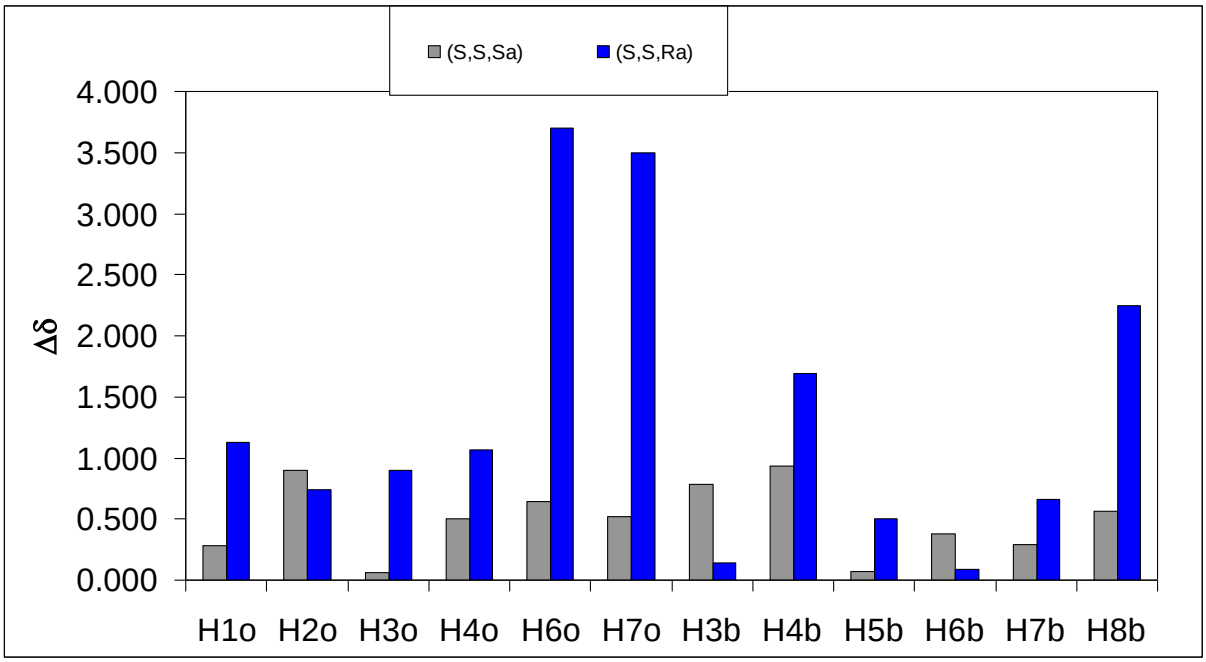

Figure S3. Differences between experimental and calculated LIS (ppm) for the (S,S,S_a) and (S,S,R_a) isomers of **9-Yb**.

5 UV/Vis Spectroscopy

Uv/vis spectra were measured in MeOH on a Jasco-V670 spectrophotometer using fluorescence quartz cuvettes (suprasil, pathlength 1.0 cm).

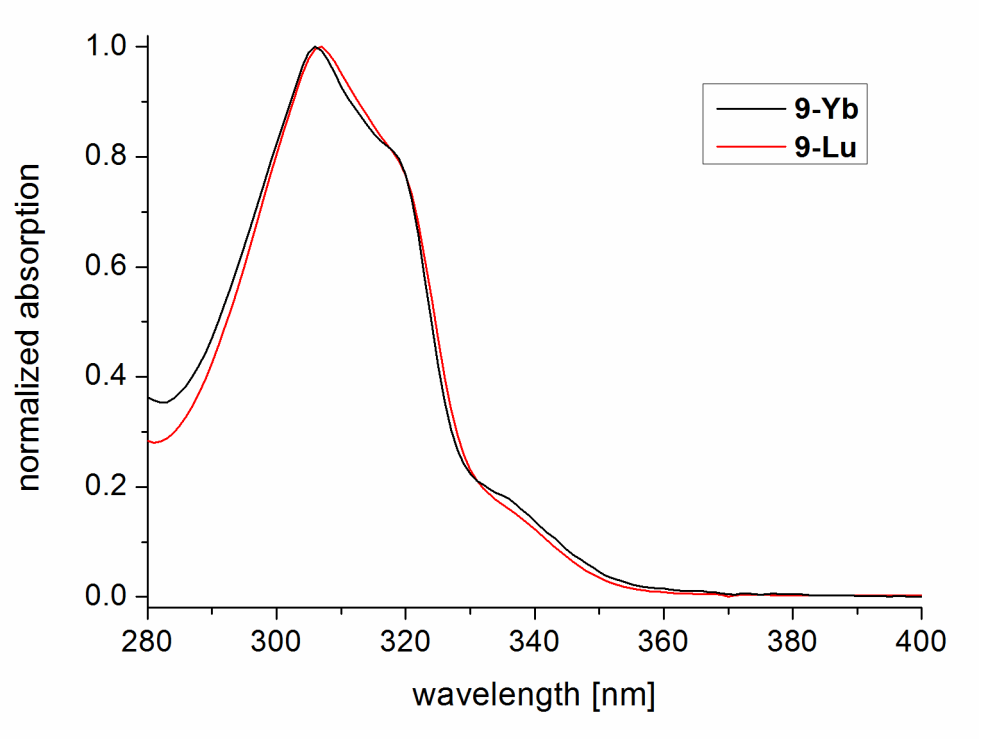

Figure S4. Normalized UV/vis absorption spectra of **9-Ln** in MeOH.

Molar extinction coefficients were determined for **9-Lu** in MeOH:

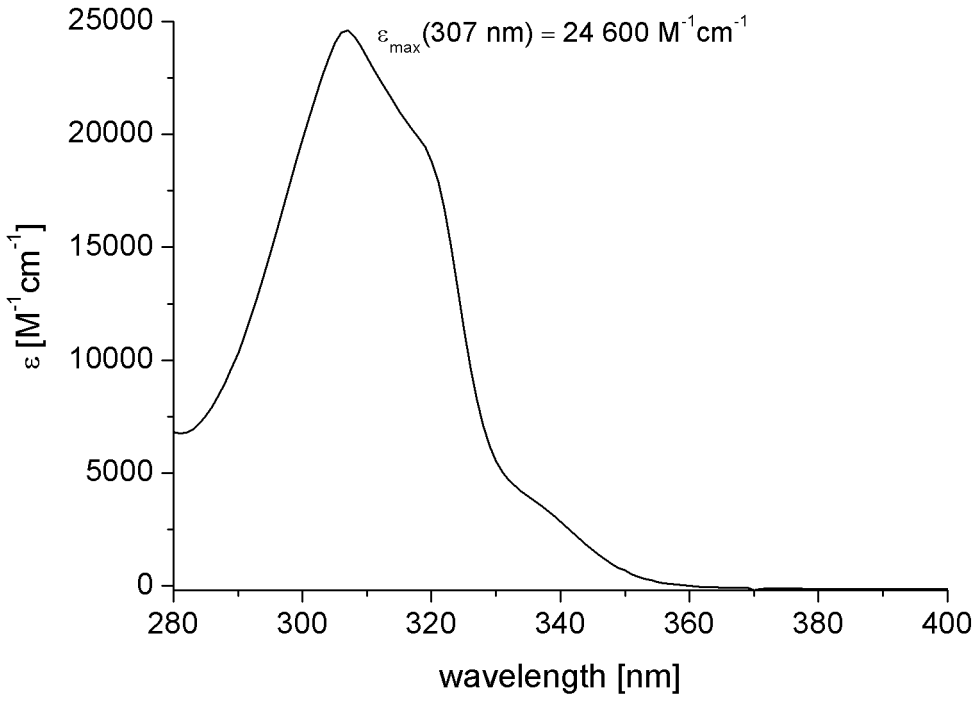

Figure S5. UV/vis absorption spectrum of **9-Lu** in MeOH.

6 Luminescence Spectroscopy

Steady state emission spectra were acquired on a PTI Quantamaster QM4 spectrofluorimeter using fluorescence quartz cuvettes (suprasil, pathlength 1.0 cm) at room temperature. CD_3OD was NMR grade (99.8%D), CH_3OH was dry, analytical grade. The excitation light source was a 75 W continuous xenon short arc lamp. Emission was monitored at 90° using a PTI P1.7R detector module (Hamamatsu PMT R5509-72 with a Hamamatsu C9525 power supply operated at -1500 V and a Hamamatsu liquid N_2 cooling unit C9940 set to -80°C). For the near-IR steady state emission measurement, a long-pass filter RG-780 (Schott, 3.0 mm thickness, transmission >83% between 800-850 nm and >99% between 850-1700 nm) was used in the excitation channel in order to avoid higher order excitation light. Spectral selection was achieved by single grating monochromators (excitation: 1200 grooves/mm, blazed at 300 nm; near-IR emission: 600 grooves/mm, blazed at 1200 nm). Luminescence lifetimes were determined with the same instrumental setup. No long-pass filter was used. The light source for these measurements was a xenon flash lamp (Hamamatsu L4633: 10 Hz repetition rate, pulse width ca. 1.5 μs FWHM). Lifetime data analysis (deconvolution, statistical parameters, etc.) was performed using the software package FeliX32 from PTI. Lifetimes were determined by deconvolution of the decay profiles with the instrument response function which was determined using a dilute aqueous dispersion of colloidal silica (Ludox® AM-30). All measured values are averages of at least three independent experiments.

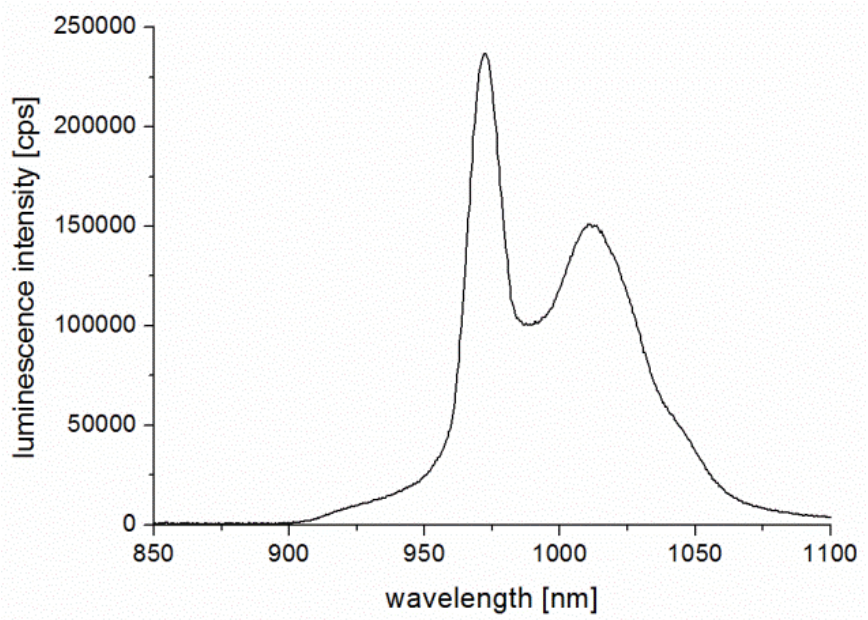

Figure S6. Steady state emission spectrum ($^2F_{5/2} \rightarrow {}^2F_{7/2}$ transition) of **9-Yb** in CD_3OD (λ_{exc} = 306 nm).

7 References

1 M. Casalino, V. De Felice, N. Fraldi, A. Panunzi, F. Ruffo, *Inorg. Chem.*, 2009, **48**, 5913.

2 C. Doffek, N. Alzakhem, C. Bischof, J. Wahsner, T. Güden-Silber, J. Lügger, C. Platas-Iglesias, M. Seitz, *J. Am. Chem. Soc.*, 2012, **134**, 16413.

3 Tao, J. M.; Perdew, J. P.; Staroverov, V. N.; Scuseria, G. E.; *Phys. Rev. Lett.* 2003, **91**, 146401.

4 Gaussian 09 (Revision A.01): Frisch, M. J.; Trucks, G. W.; Schlegel, H. B.; Scuseria, G. E.; Robb, M. A.; Cheeseman, J. R.; Scalmani, G.; Barone, V.; Mennucci, B.; Petersson, G. A.; Nakatsuji, H.; Caricato, M.; Li, X.; Hratchian, H. P.; Izmaylov, A. F.; Bloino, J.; Zheng, G.; Sonnenberg, J. L.; Hada, M.; Ehara, M.; Toyota, K.; Fukuda, R.; Hasegawa, J.; Ishida, M.; Nakajima, T.; Honda, Y.; Kitao, O.; Nakai, H.; Vreven, T.; Montgomery, Jr., J. A.; Peralta, J. E.; Ogliaro, F.; Bearpark, M.; Heyd, J. J.; Brothers, E.; Kudin, K. N.; Staroverov, V. N.; Kobayashi, R.; Normand, J.; Raghavachari, K.; Rendell, A.; Burant, J. C.; Iyengar, S. S.; Tomasi, J.; Cossi, M.; Rega, N.; Millam, N. J.; Klene, M.; Knox, J. E.; Cross, J. B.; Bakken, V.; Adamo, C.; Jaramillo, J.; Gomperts, R.; Stratmann, R. E.; Yazyev, O.; Austin, A. J.; Cammi, R.; Pomelli, C.; Ochterski, J. W.; Martin, R. L.; Morokuma, K.; Zakrzewski, V. G.; Voth, G. A.; Salvador, P.; Dannenberg, J. J.; Dapprich, S.; Daniels, A. D.; Farkas, Ö.; Foresman, J. B.; Ortiz, J. V.; Cioslowski, J.; Fox, D. J. Gaussian, Inc., Wallingford CT, 2009.

5 M. Dolg, H. Stoll, H.; A. Savin, H. Preuss, *Theor. Chim. Acta*, 1989, **75**, 173.

6 a) L. Maron, L.; O. Eisenstein, *J. Phys. Chem. A*, 2000, **104**, 7140; b) O. Eisenstein, L. Maron, L.; *J. Organomet. Chem.,* 2002, **647**, 190.

7 C. Platas-Iglesias, A. Roca-Sabio, M. Regueiro-Figueroa, D. Esteban-Gómez, A. de Blas, T. Rodríguez-Blas, *Current Inorg. Chem.*, 2011, **1**, 91.

8 C. Platas-Iglesias, *Eur. J. Inorg. Chem.*, 2012, **105**, 2023.

9 J. Tomasi, B. Mennucci, R. Cammi, *Chem. Rev.*, 2005, **105**, 2999.